Available online at http://journal-of-agroalimentary.ro

Journal of Agro-alimentary Processes and Technologies 2024, 30 (2), 136-141

Journal of Agroalimentary Processes and Technologies

Obtaining and characterization of doped lanthanum manganite through an unconventional method

Adina Căta[1], Antonina Lazăr[1], Ioana M.C. Ienașcu[1,2], Nick Samuel Țolea[1], Daniel Ursu[1], Anamaria Dabici[1], Paula Sfîrloagă[1,3*]

[1]National Institute of Research and Development for Electrochemistry and Condensed Matter, Dr. A. P. Podeanu 144, 300569, Timişoara, Romania
[2]"Vasile Goldiş" Western University of Arad, Faculty of Pharmacy, Liviu Rebreanu 86, 310045, Arad, Romania
[3]Spin-off Nattive-Senz SRL,Dr. A.P. Podeanu street, No. 144, 300569, Timisoara, Timis, Romania

**Corresponding author: paulasfirloaga@gmail.com*

Abstract
Considering the growing concern for food safety, the development of fast detection methods with high sensitivity and repeatability of specific food constituents is a huge necessity. In this regard, the electrochemical methods can be an effective way due to certain advantages such as low cost, fast response signal, high sensitivity and ease of use. The detection efficiency of electrochemical sensors mainly depends on the electrochemical characteristics of the electrode materials. Perovskite-based materials are ideal candidates for the development of electrochemical sensors due to their excellent catalytic activity and redox properties. We report herein the synthesis, morpho-structural properties, and electrical performance assessment of Ca doped lanthanum manganite by ultrasonic method with immersed sonotrode in the reaction medium. X-ray diffraction (XRD) and scanning electron microscopy (SEM) analyses were performed on the synthesized samples. The results indicated a well-crystallized perovskite-type structure, and 29 nm average crystallite sizes. The electron microscopy images showed that the presence of the dopant influenced the surface morphology.
Keywords: lanthanum manganite, doped, electrical properties.

1. Introduction

Materials that crystallize in the perovskite crystal structure are common crystals, currently used for many applications, including transistors, solar cells, light-emitting devices, catalysts and superconductors [1]. On the basis of the general formula ABX3, the perovskite-type materials are a family of inorganic compounds with similar crystallographic compositions and a variety of different chemical compositions, where A typically represents an alkali or alkaline earth metal cation (La, Sm, Pr) and B represents a transition metal cation (e.g., Fe, Ni, Mn, Co, Cu or Ti) [2]. Because of their diversity and interest, they have received a lot of attention from researchers in different scientific fields such as chemistry, physics and materials science. In addition, the possibility of tuning their composition and morphology to enhance their optical properties [3], magnetic responses [4], catalytic activity [5], band gaps [6] adsorption capacities [7] and electrical conductivities [8] is another important characteristic of these materials that makes them attractive for research. From the various rare earth metal cations, lanthanum offers the highest catalytic activity, which is partly attributed to the higher electrical conductivity

DOI: 10.59463/JAPT.2024.2.05

of this material [9]. LaMnO3 exhibits many fascinating chemical and physical characteristics, especially when the A or B ions are partially substituted; the crystalline structure remains essentially unchanged, whereas the performance is improved. Due to these facts is has been widely used in many fields such as supercapacitors [2], sensors [10], catalytic oxidation [11] and photocatalysis [12].

The excellent catalytic activity and redox properties of perovskite-based materials make them great candidates for the development of electrochemical sensors [13]. Perovskite-based sensors can be used to detect pathogens, allergens or contaminants in food products, thereby ensuring food safety and quality [14]. In recent decades, there has been an increased interest in the development of non-enzymatic electro-chemical sensors combined with various nanomaterials, with high sensitivity, good selectivity and low detection limit [15]. The electrochemical detection of glucose and/or hydrogen peroxide is widely studied and is used as evaluation criteria for comparing the performance of different sensors [15].

Felix et al. [16] have developed a sensor material based on lanthanum manganese oxide and functionalized carbon nanofibers for the sensitive detection of roxarsone, a pentavalent arsenic compound used as feed additive in poultry for rapid growth. The obtained composite showed good reproducibility, exceptional stability and reliable practical application in the analysis of tap water and food sample. Govindasamy et al. [17] used a La-based perovskite to prepare a sensor for the electrochemical detection of nitrite in meat extract and drinking water. The proposed electrode demonstrated excellent selectivity, repeatability, repro-ductibility, storage, and operational stability. Also, La-based perovskites were used to develop high-performance non-enzymatic sensors for detection of glucose and hydrogen peroxide, widely used as oxidant in the chemical and food industries [18-20].

In recent years, there is a growing concern regarding the use of synthetic dyes (e.g. Allura Red AC, tartrazine, Brilliant Blue FCF, Fast Green FCF, Metanil yellow) in the food industry due to their harmful effects on human health and the environment. Among the various methods used for the degradation of toxic food dyes, photocatalytic degradation has emerged as an effective and eco-friendly method for the removal of these dyes from wastewater [21]. Perovskite-type materials have been reported to have promising results in photocatalytic degradation of organic dyes [22,23]. Promising results regarding the catalytic and photocatalytic activity of some La-based perovskite materials for the removal of methyl orange from aqueous solutions have already been obtained and reported in a previous work [24].

The present work focuses on the preparation and morpho-structural characterization of undoped and Ca doped LaMnO3-type perovskite materials with potential use in sensing applications for the detection of various analytes related to food safety, and also in the photocatalytic degradation of toxic food dyes.

1. Materials and method

All the reagents were of high purity and were purchased from Aldrich. Undoped and Ca doped lanthanum manganite were prepared by ultrasonic method with immersed sonotrode in the reaction medium. The starting materials for the synthesis of Ca-$LaMnO_3$ were $La(NO_3)_3 \cdot 6H_2O$, Mn $(NO_3)_2$, $Ca(NO3)_2 \cdot 4H_2O$, $Ca(NO_3)_2 \cdot 4H_2O$ and NaOH were used. The materials were synthesized according to the procedure described in the paper by Sfirloaga [25]. The obtained gel was washed with water and ethanol to remove secondary products and then dried at 100 °C for 1 h. The powder was heat treated at 600°C for 6 h.

X-ray diffraction (XRD) by means of a PANalytical diffractometer, with Cu-Kα radiations (λ = 0.15406 nm) in a 2θ range from 20° to 80°, and a scan rate of 2°/min was used for the study of the crystalline phase, and a scanning electron microscope (SEM) Inspect S was used to inspect the surface morphology of the obtained materials. Moreover, electrical conductivity measurements were performed at temperatures between 30°C and 120°C with an E4980A RLC-meter (Agilent).

2. Results and discussion

3.1. XRD Analysis

X-ray powder diffraction patterns of the obtained samples by ultrasonic method are

presented in Figure 1. The studied materials exhibit a well crystallized perovskite-type structure, and the structural parameters were refined using the X′PertHighScore Plus software, using CIF 1521153.crystalline phase.

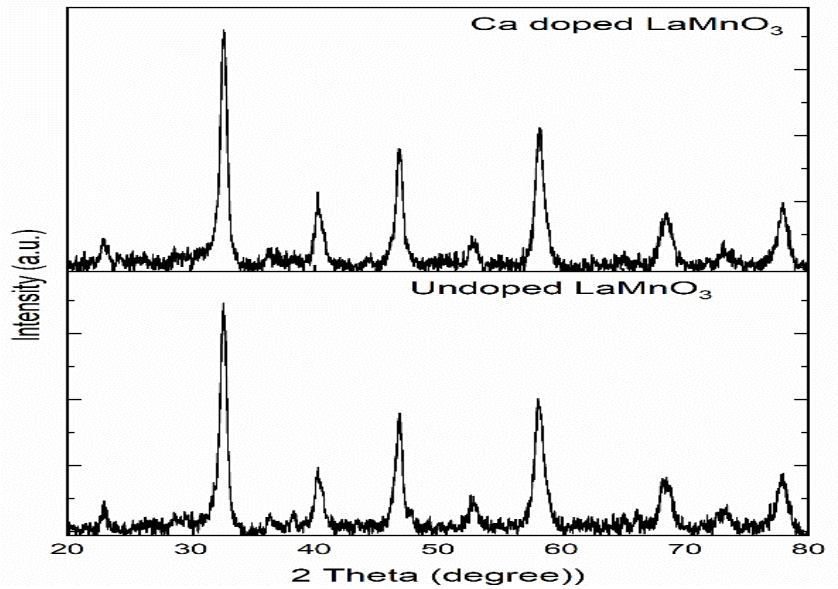

Figure 1. XRD patterns for undoped and Ca doped $LaMnO_3$

3.2. SEM investigations

SEM images of undoped and Ca-doped LaMnO3 are shows in Figure 2. The materials were analyzed in high vacuum working mode, using the ETD detector, at 40000X magnification.

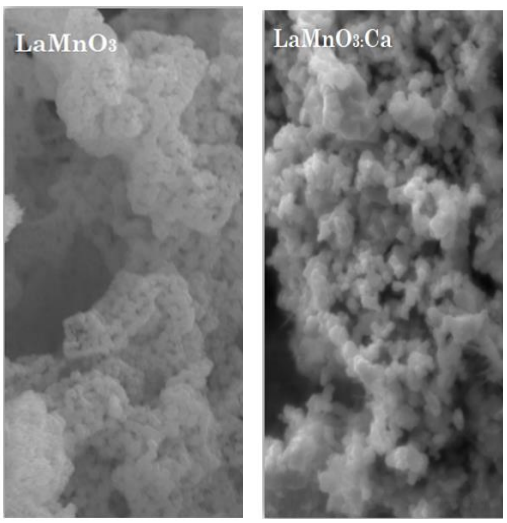

Figure 2. SEM image for undoped and Ca-doped $LaMnO_3$

As can be seen from the surface morphology, undoped lanthanum manganite is heavily agglomerated in asymmetric formations, having a sponge-like appearance. In the case of Ca doped perovskite material, it can be observed that, although the particles are agglomerated, they are in the form of cubes. Consequently, it can be concluded that the presence of the dopant influenced the morphology of the particles.

3.3. Electrical properties

In Figure 3 are presented the frequency dependence of the real Z' and imaginary Z" components of the complex impedance.

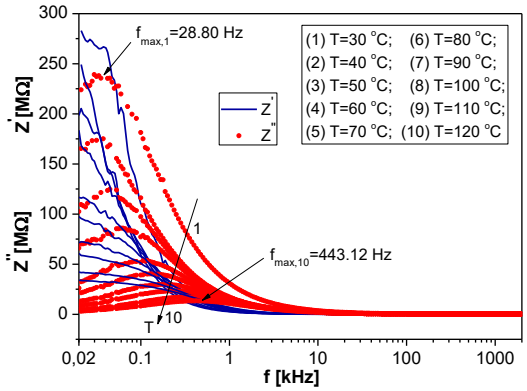

Figure 3. Frequency dependence of the real Z' and imaginary Z" components of the complex impedance at different temperatures for Ca-doped $LaMnO_3$

From Figure 4, by fitting with a straight line and assuming that the relaxation time varies according to Arrhenius law, the activation

energy due to the relaxation processes for each sample is obtained.

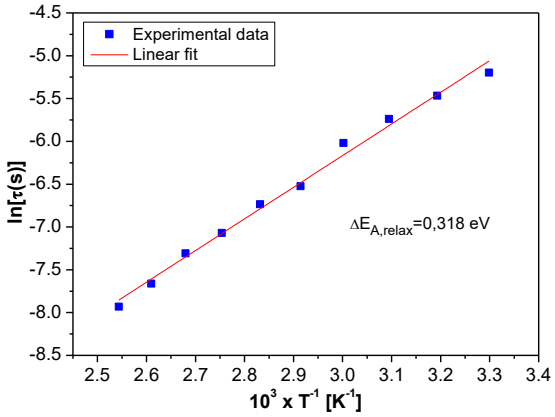

Figure 4. Dependence of lnτ on T^{-1} for Ca-doped $LaMnO_3$

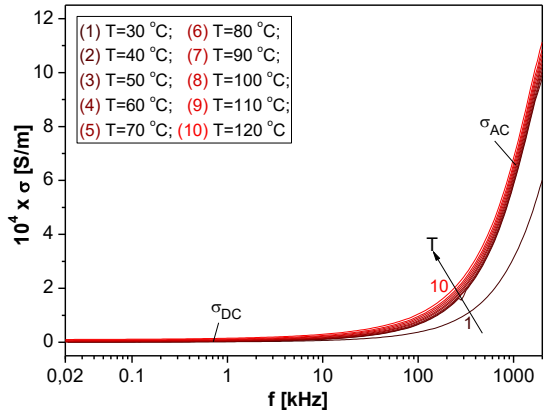

Figure 5. Frequency dependence of total conductivity σ at different temperatures for Ca-doped $LaMnO_3$

It is known that the total conductivity is as follows:

$$\sigma = \sigma_{DC}(T) + \sigma_{AC}(\omega, T) \quad (1)$$

where $\sigma_{DC}(T)$ is the DC component of the electrical conductivity. It does not depend on the frequency; it depends only on the temperature. In static field or low frequency range, it is assumed that the hopping process would be determined by Mott's variable-range-hopping (VRH) mechanism [26] and the static conductivity, σ_{DC}, is given by the following expression:

$$\sigma_{DC} = \sigma_0 \exp\left[-(T_0/T)^{1/4}\right] \quad (2)$$

where T_0 is characteristic temperature coefficient being a measure of the degree of disorder, given by the relation:

$$T_0 = \frac{\lambda a^3}{kN(E_F)} \quad (3)$$

In Eq. (3), $\lambda \cong 16.6$, is a dimensionless constant; $\alpha \cong 10^{-7}$ cm represents the degree of localization and $N(E_F)$ is the density of the localized states at the Fermi level E_F. The hopping distance, R is given by the relation,

$$R = \left(\frac{9}{8\alpha kTN(E_F)}\right)^{1/4} \quad (4)$$

and the hopping energy W is given by the relation [27]

$$W = \frac{3}{4\pi R^3 N(E_F)} \quad (5)$$

The second term $\sigma_{AC}(\omega, T)$ from equation (1), depends on frequency and temperature being correlated to the dielectric relaxation processes determined by localized electric charge carriers. This component $\sigma_{AC}(\omega, T)$ obeys of a Jonscher power law [28], which tries to explain the behavior of the AC electrical conductivity, having the following expression:

$$\sigma_{AC}(\omega, T) = A(T)\omega^{n(T)} \quad (6)$$

where $A(T)$ is a parameter depending on temperature and the exponent parameter n is a non-dimensional temperature dependent parameter.

Next figure presents the Mott's VRH plot, $ln\sigma_{DC}$ versus $(1/T)^{1/4}$ for Ca-doped lanthanum manganite sample, using the Eq. (2).

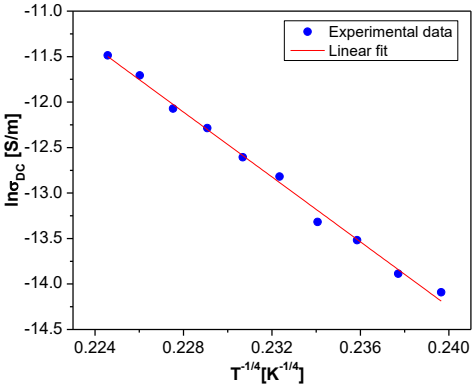

Figure 6. $ln\sigma_{DC}$ versus $(1/T)^{1/4}$ for Ca-doped $LaMnO_3$

By fitting the experimental dependence, $\ln\sigma(T^{-1/4})$ from figure 6, to the linear equation, one obtains the parameters, T_0, corresponding to Ca-doped lanthanum manganite sample. Using the values obtained for T_0 and eq. (3), we have computed the density of the localized states at the Fermi level, $N(E_F)$ and the values obtained are shown in table 1. From equation (4) and using the computed values of $N(E_F)$, we have

determined the average hopping distance, *R*, corresponding to the sample, at each temperature within the range 300 – 393 K. Knowing the hopping distance *R* and using equation (5) we have computed the hopping energy *W* for the sample. The values obtained for the parameters *R* and *W*, corresponding to the Ca doped $LaMnO_3$, at three temperatures, are shown in Table 1.

Table 1. Mott parameter values

Sample	T_0 [K]	$N(E_F)$ [$cm^{-3}·eV^{-1}$]	R [nm]			W [meV]		
			303 K	353 K	393 K	303 K	353 K	393 K
Ca-doped $LaMnO_3$	0.101×10^{10}	1.90×10^{17}	21.79	20.98	20.42	121	136	147

From figure 7, considering that at high frequencies the CBH model of conductivity is applicable, it follows that $1–n=6kT/W_m$ (where W_m is the bandgap energy of the material), by fitting we obtain the W_m value the sample.

Considering the obtained results regarding the physico-chemical characterization and electrical properties of $LaMnO_3$-type perovskite materials, it can be concluded that the studied compounds could be tested in further studies as sensitive materials for the detection of various analytes related to food safety.

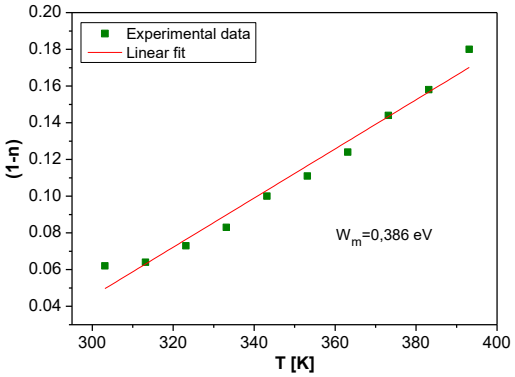

Figure 7. Temperature dependence of the deviation from unity of the exponent (1-n) for Ca-doped $LaMnO_3$

4. Conclusions

In this work, undoped and Ca doped lanthanum manganite were synthesized by means of ultrasonic method with immersed sonotrode in the reaction medium followed by heat treatment at 600°C. The obtained materials were found to be phase pure, with crystallites of about 30 nm. The morphological analysis of the surface highlighted the influence of the dopant on the shape of the particles. In further studies, we are considering testing these materials as such or in various combinations both as electrode materials for the detection of some food contaminants or components in food products and as catalysts in photocatalytic degradation of some toxic food dyes from wastewater.

Acknowledgements

This work was supported by the POC/1025/1/3, Cod SMIS 2014+ 156350. The authors thank to Prof. I. Malaescu and Prof. C.N.Marin for materials characterization.

References

1. Aïssa, B.; Ali, A.; El-Mellouli, F., Oxide and Organic–Inorganic Halide Perovskites with Plasmonics for Optoelectronic and Energy Applications: A Contributive Review, *Catalysts* **2021**, *11*(9), 1057.
2. Deshmukh V.V.; Harini, H.V.; Nagaswarupa, H.P.; Naik, R.; Ravikumar, C.R., Development of novel Co^{3+} doped $LaMnO_3$ perovskite electrodes for supercapacitors and sensors: Mechanism of electrochemical energy storage and oxygen intercalation, *Journal of Energy Storage* **2023**, *68*, 107805.
3. Mishra, S.; Choudhary, R.N.P.; Parida, S.K., Structural, dielectric, electrical and optical properties of a double perovskite: $BaNaFeWO_6$ for some device applications, *Journal of Molecular Structure* **2022**, *1265*, 133353.
4. Trukhanov, A.V.; Turchenko, V.O.; Bobrikov, I.A.; Trukhanov, S.V.; Kazakevich, I.S.; Balagurov, A.M., Crystal structure and magnetic properties of the $BaFe_{12-x}Al_xO_{19}$ (x=0.1–1.2) solid solutions, *Journal of Magnetism and Magnetic Materials* **2015**, *393*, 253-259.
5. Kozlovskiy, A.L.; Zdorovets, M.V., The study of the structural characteristics and catalytic activity of $Co/CoCo_2O_4$ nanowires, *Composites Part B: Engineering* **2020**, *191*, 107968.
6. Pascale, F.; Pastore, M.; Doll, K.; Dovesi, R., On the role of the exact Hartree–Fock exchange in determining the Jahn–Teller energy splitting and electronic band gap in the KBF_3 (B=Sc, Ti, Fe, Co, Cr and Cu) perovskites. A quantum

mechanical investigation, *Chemical Physics Letters* **2024**, *836*, 141053.
7. Zhou, M.; Ma, X.; Ji, C.; Zhao, L.; Chen, J.; Shi, Y.; Liu, D.; Zhong, Z.; Low, Z.-X.; Xing, W., Chelating adsorption-engaged anionic dye removal and Fenton-driven regeneration in ferromagnetic Ti/Co-$LaFeO_3$ perovskite, *Chemical Engineering Journal* **2024**, *479*, 147600.
8. Wang, P.-J.; Zhou, D.; Li, J.; Pang, L.-X.; Liu, W.-F.; Su, J.-Z.; Singh, C.; Trukhanov, S.; Trukhanov, A., Significantly enhanced electrostatic energy storage performance of P(VDF-HFP)/$BaTiO_3$-$Bi(Li_{0.5}Nb_{0.5})O_3$ nanocomposites, *Nano Energy* **2020**, *78*, 105247.
9. Flores-Lasluisa, J.X.; Huerta, F.; Cazorla-Amoros, D.; Morallon, E., Manganese oxides/$LaMnO_3$ perovskite materials and their application in the oxygen reduction reaction, *Energy* **2022**, *247*, 123456.
10. Zhang, J.; Chen, Y.; Li, L.; Chen, X.; An, W.; Qian, X.; Tao, Y., $LaMnO_3$/Co_3O_4 nanocomposite for enhanced triethylamine sensing properties, *Journal of Rare Earths* **2024**, *42*, 733-742.
11. Zhang, C.; Wang, C.; Hua, W.; Guo, Y.; Lu, G.; Gil, S.; Giroir-Fendler, A., Relationship between catalytic deactivation and physicochemical properties of $LaMnO_3$ perovskite catalyst during catalytic oxidation of vinyl chloride, *Applied Catalysis B: Environmental* **2016**, *186*, 173-183.
12. Luo, H.; Guo, J.; Shen, T.; Zhou, H.; Liang, J.; Yuan, S., Study on the catalytic performance of $LaMnO_3$ for the RhB degradation, *Journal of the Taiwan Institute of Chemical Engineers* **2020**, *109*, 15-25.
13. Valenzuela-Amaro, H.M.; Aguayo-Acosta, A.; Meléndez-Sánchez, E.R.; de la Rosa, O.; Vázquez-Ortega, P.G.; Oyervides-Muñoz, M.A.; Sosa-Hernández, J.E.; Parra-Saldívar, R., Emerging Applications of Nanobiosensors in Pathogen Detection in Water and Food, *Biosensors* **2023**, *13*, 922.
14. Korde, V.B.; Khot, S.; Kamble, D.B.; Amalraj, S., Review: Perovskite nanostructures materials versatile platform for advance biosensor applications, *Sensors and Actuators Reports* **2024**, *7*, 100201.
15. He, J.; Xu, X.; Li, M.; Zhou, S., Zhou W. Recent advances in perovskite oxides for non-enzymatic electrochemical sensors: A review, *Analytica Chimica Acta* **2023**, *1251*, 341007.
16. Felix, M.A.J.; Shanlee, S.S.R.; Chen, S.-M.; Ruspika, S.; Balaji, R.; Chandrasekar, N., Design and fabrication of La-based perovskites incorporated with functionalized carbon nanofibers for the electrochemical detection of roxarsone in water and food samples, *Analytical Methods* **2024**, *16*, 2857-2868.
17. Govindasamy, M.; Wang, S.-F.; Huang, C.-H.; Alshgari, R.A.; Ouladsmane, M., Colloidal synthesis of perovskite-type lanthanum aluminate incorporated graphene oxide composites: Electrochemical detection of nitrite in meat extract and drinking water in the development of a sensor with applicability, *Microchimica Acta* **2022**, *189*, 210.
18. Wang, Y.-Z.; Zhong, H.; Li, X.-M.; Jia, F.-F.; Shi, Y.-X.; Zhang, W.-G.; Cheng, Z.-P.; Zhang, L.-L.; Wang, J.-K., Perovskite $LaTiO_3$–Ag0.2 nanomaterials for nonenzymatic glucose sensor with high performance, *Biosensors and Bioelectronics* **2013**, *48*, 56–60.
19. Xu D., Li L., Ding Y., Cui S. Electrochemical hydrogen peroxide sensors based on electrospun $La_{0.7}Sr_{0.3}Mn_{0.75}Co_{0.25}O_3$ nanofiber modified electrodes, *Analytical Methods* **2015**, *7*, 6083.
20. He, J.; Sunarso, J.; Zhu, Y.; Zhong, Y.; Miao, J.; Zhou, W.; Shao, Z., High-performance non-enzymatic perovskite sensor for hydrogen peroxide and glucose electrochemical detection, *Sensors and Actuators B* **2017**, *244*, 482-491.
21. Khan, K.A.; Shah, A.; Nisar, J.; Haleem, A.; Shah, I., Photocatalytic Degradation of Food and Juices Dyes via Photocatalytic Nanomaterials Synthesized through Green Synthetic Route: A Systematic Review, *Molecules* **2023**, *28*, 4600.
22. Rojas-Cervantes, M.L.; Castillejos, E., Perovskites as Catalysts in Advanced Oxidation Processes for Wastewater Treatment, *Catalysts* **2019**, *9*, 230.
23. Mahmoudi, F.; Saravanakumar, K.; Maheskumar, V.; Njaramba, L.K.; Yoon , Y.; Park, C.M., Application of perovskite oxides and their composites for degrading organic pollutants from wastewater using advanced oxidation processes: Review of the recent progress, *Journal of Hazardous Materials* **2022**, *436*, 129074.
24. Sfirloaga, P.; Ivanovici, M.-G.; Poienar, M.; Ianasi, C.; Vlazan, P., Investigation of Catalytic and Photocatalytic Degradation of Methyl Orange Using Doped $LaMnO_3$ Compounds, *Processes* **2022**, *10*, 2688.
25. Sfirloaga, P.; Poienar, M.; Ianasi, C.; Vlase, T.; Vlazan, P., Synthesis and morpho-structural characterization of $NaTaO_3$ nanomaterials obtained by ultrasonic method with immersed sonotrode, *Journal of Thermal Analysis and Calorimetry* **2017**, *127*, 457–462.
26. Mott, N.F.; Davis, E.A., *Electronic Processes in Noncrystalline Materials*, 2nd ed., Clarendon Press, Oxford, 1979, pp. 32-36.
27. Davis, E.A.; Mott, N.F., Conduction in non-crystalline systems V. Conductivity, optical absorption and photoconductivity in amorphous semiconductors, *The Philosophical Magazine* **1970**, *22*, 903-922.
28. Jonscher, A.K., *Universal relaxation law: a sequel to Dielectric relaxation in solids*, Chelsea Dielectrics Press, London, 1996, pp. 198–200.